

## First insight into human extrahepatic metabolism of flame retardants

Abdallah, Mohamed Abou-Elwafa; Nguyen, Khanh-Hoang; Moehring, Thomas; Harrad, Stuart

DOI:

[10.1016/j.chemosphere.2019.04.017](https://doi.org/10.1016/j.chemosphere.2019.04.017)

License:

Creative Commons: Attribution-NonCommercial-NoDerivs (CC BY-NC-ND)

*Document Version*

Peer reviewed version

*Citation for published version (Harvard):*

Abdallah, MA-E, Nguyen, K-H, Moehring, T & Harrad, S 2019, 'First insight into human extrahepatic metabolism of flame retardants: biotransformation of EH-TBB and Firemaster-550 components by human skin subcellular fractions', *Chemosphere*, vol. 227, pp. 1-8. <https://doi.org/10.1016/j.chemosphere.2019.04.017>

[Link to publication on Research at Birmingham portal](#)

### **Publisher Rights Statement:**

Checked for eligibility: 28/06/2019

### **General rights**

Unless a licence is specified above, all rights (including copyright and moral rights) in this document are retained by the authors and/or the copyright holders. The express permission of the copyright holder must be obtained for any use of this material other than for purposes permitted by law.

- Users may freely distribute the URL that is used to identify this publication.
- Users may download and/or print one copy of the publication from the University of Birmingham research portal for the purpose of private study or non-commercial research.
- User may use extracts from the document in line with the concept of 'fair dealing' under the Copyright, Designs and Patents Act 1988 (?)
- Users may not further distribute the material nor use it for the purposes of commercial gain.

Where a licence is displayed above, please note the terms and conditions of the licence govern your use of this document.

When citing, please reference the published version.

### **Take down policy**

While the University of Birmingham exercises care and attention in making items available there are rare occasions when an item has been uploaded in error or has been deemed to be commercially or otherwise sensitive.

If you believe that this is the case for this document, please contact [UBIRA@lists.bham.ac.uk](mailto:UBIRA@lists.bham.ac.uk) providing details and we will remove access to the work immediately and investigate.

**First Insight into Human Extrahepatic Metabolism of Flame  
Retardants: Biotransformation of EH-TBB and Firemaster-550  
components by Human Skin Subcellular Fractions**

*Mohamed Abou-Elwafa Abdallah<sup>1,2\*</sup>, Khanh-Hoang Nguyen<sup>1</sup>, Thomas Moehring<sup>3</sup>, Stuart  
Harrod<sup>1</sup>*

<sup>1</sup> School of Geography, Earth and Environmental Sciences, University of Birmingham,  
Birmingham, B5 2TT, United Kingdom.

<sup>2</sup>Department of Analytical Chemistry, Faculty of Pharmacy, Assiut University,  
71526 Assiut, Egypt

<sup>3</sup> Thermo Fisher Scientific (GmbH) Bremen, Hanna-Kunath-Str. 11, 28199 Bremen, Germany

\* Corresponding author

E-mail: M.abdallah@bham.ac.uk

Tel.: +44 121 414 5527

## Abstract

2-ethylhexyl-2,3,4,5-tetrabromobenzoate (EH-TBB) and a mixture of EH-TBB, Bis(2-ethylhexyl)tetrabromophthalate (BEH-TEBP) and Triphenyl phosphate (TPhP), prepared in a ratio similar to the Firemaster-550™ (FM550) flame retardant formulation, were exposed to human skin subcellular fractions (S9) to evaluate their dermal *in vitro* metabolism for the first time. After 60 mins of incubation, tetrabromobenzoic acid (TBBA) and diphenyl phosphate (DPhP) were identified as the major metabolites of EH-TBB and TPhP, respectively using UPLC-Q-Exactive Orbitrap™-MS analysis. Dermal biotransformation of EH-TBB and TPhP was catalyzed by skin carboxylesterases rather than CYP450 enzymes, while no stable metabolites could be identified for BEH-TEBP. Metabolite formation rates of EH-TBB as individual compound and as a component of FM550 fitted the Michaelis-Menten model, while no steady state could be reached for TPhP under experimental conditions. Estimated maximum metabolic rate ( $V_{\max}$ ) for TBBA formation upon exposure to FM550 was lower than  $V_{\max}$  for EH-TBB (1.08 and 15.2 pmol min<sup>-1</sup> mg protein<sup>-1</sup>, respectively). This indicates dermal metabolism would contribute less to the clearance of EH-TBB body burden than hepatic metabolism ( $V_{\max} = 644$  pmol min<sup>-1</sup> mg protein<sup>-1</sup>). Implications for human exposure include EH-TBB accumulation in skin tissue and human exposure to dermal metabolic products, which may have different toxicokinetic and toxicodynamic parameters than parent flame retardants.

**Keywords:** *Flame retardants; Firemaster 550; EH-TBB; dermal metabolism; human exposure.*

## Introduction

2-ethylhexyl-2,3,4,5-tetrabromobenzoate (EH-TBB) is an additive flame retardant produced by Chemtura™ Corporation. It is available in 2 commercial mixtures: Firemaster 550™ (FM550) and Firemaster BZ-54™ (FMBZ-54). In FM550, EH-TBB is mixed with bis(2-ethylhexyl) tetrabromophthalate (BEH-TEBP), triphenyl phosphate (TPhP) and assorted isopropyl triphenylphosphate (ITP) isomers in the ratio: 36% EH-TBB, 14% BEH-TEBP, 18% TPhP and 32% ITPs by weight (Belcher et al., 2014). As additive FRs, EH-TBB and the other components of FM550 may leach out from treated consumer goods and contaminate the environment. They have been detected globally in various environmental matrices including indoor dust,(Carignan et al., 2013; Tao et al., 2016; Hammel et al., 2017) indoor air,(Cequier et al., 2014; Tao et al., 2016) outdoor air,(Ma et al., 2012) chicken eggs,(Zheng et al., 2016) aquatic biota (Strid et al., 2013) and foodstuffs (Xu et al., 2015). Similar to other emerging FRs, the environmental occurrence of EH-TBB and FM550 components is expected to be mainly in indoor dust. Residential dust in the UK contained median concentrations of EH-TBB and BEH-TEBP at 4 - 23 (median = 5.8) and 80 - 3187 (median = 320) ng/g, respectively (Al-Omran and Harrad, 2016). In the U.S.A., house dust samples from California collected in 2011 showed higher levels of FM550 components than those collected in 2006. Specifically, concentration ranges of EH-TBB and BEH-TEBP in 2011 were 45-5900 (median = 100) and <2-3800 (median = 260) ng/g, while those in 2006 were 4-740 (median = 48) and 36-1900 (median = 140), respectively (Dodson et al., 2012). Extremely high concentrations of EH-TBB and BEH-TEBP were reported in dust from an American gymnasium ranging from 20,800 to 85,600 (median = 28,900) ng/g for EH-TBB and 17,300 to 44,900 (median = 30,000) ng/g for BEH-TEBP (Carignan et al., 2013). This is

69 of concern due to the potential toxicity of FM550 components to humans and wildlife. Both  
70 EH-TBB and BEH-TEBP expressed *in vitro* antiestrogenic and antiandrogenic effects in the  
71 yeast estrogen screen and yeast androgen screen assays (reflected in inhibition of  $\beta$ -  
72 galactosidase production by the assays), as well as increased oestrogen production in the  
73 human H295R steroidogenesis assays (Saunders et al., 2013). By use of primary porcine  
74 testicular cells, Mankidy et al. also investigated the effects of EH-TBB and BEH-TEBP on  
75 steroidogenesis via different mechanisms; EH-TBB induced the production of cortisol and  
76 aldosterone while BEH-TEBP promoted sex hormones synthesis (Mankidy et al., 2014).  
77 FM550-administered rats showed many negative health effects e.g. advanced female  
78 puberty, weight gain, altered exploratory behaviours and hepatic carboxylesterases activity  
79 (Patisaul et al., 2013). FM550 (mainly driven by the TPhP component) was found to bind to  
80 human peroxisome proliferator-activated receptor  $\gamma$  (PPAR $\gamma$ 1) and subsequently induced  
81 PPAR $\gamma$ 1 transcription activity. The same study also reported adipogenesis induction in  
82 primary mouse bone marrow cultures by FM550 and TPhP (Pillai et al., 2014).  
83 Accidental indoor dust ingestion is reported as a major exposure pathway of humans to  
84 EH-TBB, BEH-TBP and TPhP (Besis et al., 2017; Tao et al., 2017). However, the significance  
85 of dermal absorption as a pathway of human exposure to halogenated flame retardants via  
86 contact with contaminated dust or flame retarded consumer products has been recently  
87 highlighted (Abdallah et al., 2016; Frederiksen et al., 2016; Abdallah and Harrad, 2018;  
88 Frederiksen et al., 2018). This is of particular relevance to EH-TBB and FM550, which are  
89 widely used to flame proof upholstered furniture including childcare products (e.g. car  
90 seats and nap mats) (Hammel et al., 2017; Stubbings et al., 2018). A recent study by our  
91 research group revealed dermal uptake of some brominated FRs via contact with

upholstered furniture may even exceed exposure via dust ingestion or dietary exposure (Abdallah and Harrad, 2018). Frederiksen et al. reported on the dermal uptake of EH-TBB, BEH-TEBP and TPhP using a human skin *ex vivo* model. Based on the mass balance exercise, dermal biotransformation was suggested for all 3 flame retardants based on their ester chemical structure (Frederiksen et al., 2016; Frederiksen et al., 2018). This is supported by Hopf et al. who found that diethyl hexyl phthalate is completely hydrolysed to monoethyl hexyl phthalate by freshly excised human skin, such that only the metabolites penetrate through the skin to reach systemic circulation (Hopf et al., 2014). While it is reasonable to hypothesize that dermal exposure to EH-TBB and FM550 components via contact with furniture may be substantial, very little is known about human dermal metabolism of these flame retardants. While the hepatic metabolism of these FRs has been studied using various *in vitro* techniques, (Roberts et al., 2012; Van den Eede et al., 2013) the products and role of extrahepatic dermal metabolism of FRs remains largely unknown. Consequently, understanding of the skin biotransformation pathways, rates and products of the esterified flame retardants EH-TBB, BEH-TEBP and TPhP is important for comprehensive risk assessment of these chemicals. Against this backdrop, the current study aims to provide the first insights into the dermal biotransformation of EH-TBB, BEH-TEBP and TPhP using *in vitro* human skin S9 fractions. Specific objectives include: (a) dermal metabolite identification; (b) metabolic rate estimation for EH-TBB as a single compound (FMBZ-54) and in a mixture with BEH-TEBP and TPhP (FM550); and (c) an evaluation of the implications of dermal metabolism for human dermal exposure to the studied flame retardants.

## Materials and Methods

### Chemicals and Standards

All solvents and reagents used in this study were purchased from Fisher Scientific (Loughborough, UK) and were of HPLC grade or higher. 2-Ethylhexyl-2,3,4,5-tetrabromobenzoate (EH-TBB) and bis(2-ethylhexyl) tetrabromophthalate (BEH-TEBP) for dosing solutions (purity >95%) were obtained as neat standards from AccuStandard, Inc. (New Haven, CT, USA). High-resolution Orbitrap-MS scan of the neat standards revealed no brominated impurities/degradation products. Moreover, no effects on the metabolic activity of the human skin enzymes were observed upon exposure to the EH-TBB and BEH-TEBP standard solutions. High purity standards of EH-TBB, BEH-TEBP, triphenyl phosphate (TPhP), 2-ethylhexyl-2,3,4,5-tetrabromo[<sup>13</sup>C<sub>6</sub>]benzoate (<sup>13</sup>C-EH-TBB), bis(2-ethylhexyl-d<sub>17</sub>)-tetrabromo[<sup>13</sup>C<sub>6</sub>]phthalate (<sup>13</sup>C-BEH-TEBP), tetrabromobenzoic acid (TBBA), <sup>13</sup>C-labelled tetrabromobenzoic acid (<sup>13</sup>C-TBBA ) and α-1,2,5,6,9,10-hexabromo[<sup>13</sup>C<sub>12</sub>]cyclododecane] (<sup>13</sup>C-α-HBCDD) were purchased from Wellington Laboratories (Guelph, ON, Canada). Triphenyl phosphate-d<sub>15</sub> (TPhP-d<sub>15</sub>) and diphenyl phosphate (DPhP) were purchased from Sigma Aldrich (Dorset, UK). RapidStart™ NADPH regenerating system was purchased from XenoTech (Kansas, KS, USA), William's E medium was obtained from Thermo Fisher Scientific (Paisley, UK). Human skin S9 fractions (HS-S9) was purchased from Biopredic International (Saint Grégoire, France), comprising a pooled sample prepared from the abdominal skin of 3 white female donors after plastic surgery (age range 33-46 years – *further details are provided in the supporting information*). Individual EH-TBB dosing solutions were prepared by dissolving EH-TBB in dimethyl sulfoxide (DMSO). Firemaster 550™ (FM550)-equivalent mixtures were prepared by

dissolving EH-TBB, BEH-TEBP and TPhP in the ratio 53:20.5:26.5 by weight in DMSO, similar to the reported ratio for the technical FM550 mixture (Belcher et al., 2014). Isopropyl triphenylphosphate isomers (ITP) of sufficient high purity were not available to our lab at the time of conducting this study; hence these were not included in the FM550 dosing solutions applied in the current study. FM550 solutions were prepared such that each dosing level contained concentrations of EH-TBB similar to those in the individual EH-TBB dosing solutions.

#### *In vitro Incubation Experiments*

Pre-incubations were performed at different HS-S9 concentrations and different times. After optimization of the reaction parameters, the following exposure protocol was applied: 0.11 mg of HS-S9, William's E medium and 10  $\mu$ L of EH-TBB/FM550 dosing solutions (final concentration 10  $\mu$ M of EH-TBB) were pre-incubated for 5 minutes at 37 °C. NADPH regenerating system (final concentration: 2.0 mM nicotinamide adenine dinucleotide phosphate, 10.0 mM glucose-6-phosphate and 2 units/mL glucose-6-phosphate dehydrogenase) was added to make a final volume of 1 mL. The samples were then incubated at 37 °C, 5% CO<sub>2</sub> and 98% relative humidity for 60 min. At the end of the incubation, 1 mL of ice-cold ethyl acetate was added to stop the reaction prior to sample extraction.

#### *Sample extraction*

Incubated EH-TBB samples were spiked with 20 ng each of <sup>13</sup>C-EH-TBB and <sup>13</sup>C-TBBA while FM550 samples were spiked with 20 ng each of <sup>13</sup>C-EH-TBB, <sup>13</sup>C-TBBA, <sup>13</sup>C-BEH-TEBP and TPhP-D<sub>15</sub> as internal (surrogate) standards. Spiked samples were mixed with 3 mL of ethyl acetate by vortexing for 60 s, followed by ultrasonication for 5 min and



centrifuged at 4000 g for 5 min. The organic layer was collected and the extraction procedure was repeated twice. The combined extracts were evaporated to dryness under a gentle stream of nitrogen then reconstituted in 100  $\mu$ L of methanol containing 20 ng of  $^{13}\text{C}$ - $\alpha$ -HBCDD as a recovery determination (syringe) standard for QA/QC purposes.

### *Instrumental analysis*

Samples were analyzed on a UPLC-Orbitrap-HRMS platform (Thermo Fisher Scientific, Bremen, Germany) composed of a Dionex Ultimate 3000 liquid chromatograph composed of a HPG-3400RS dual pump, a TCC-3000 column oven and a WPS-3000 auto sampler, coupled to a Q-Exactive Plus Orbitrap mass spectrometer. Chromatographic separation was performed on an Accucore RP-MS column (100 x 2.1 mm, 2.6  $\mu$ m) with water (mobile phase A) and methanol (mobile phase B). A gradient programme at 400  $\mu$ L/min flow rate was applied as follows: start at 20% B; increase to 100% B over 9 min, held for 3 min; then decrease to 20% B over 0.1 min; maintained constant for a total run time of 15 min. The mobile phase composition and gradient were selected based on the polarity and solubility of the target compounds and their reported metabolites. Methanol is used as the organic phase because none of the target compounds or their reported metabolites (e.g. monohydroxy or dihydroxy metabolites) are freely water soluble (Roberts et al., 2012; Van den Eede et al., 2013). Orbitrap-MS data from both electrospray ionization (ESI) and atmospheric pressure chemical ionization (APCI) modes was acquired for each sample. Negative APCI was used for determination of EH-TBB,  $^{13}\text{C}$ -EH-TBB, BEH-TEBP,  $^{13}\text{C}$ -BEH-TEBP and screening for potential metabolites. The more universal, softer ESI mode was used in positive/negative alternative switching mode for screening and identification of the produced metabolites, as well as determination of TPhP and TPhP-d<sub>15</sub>. The optimized

Orbitrap-MS parameters for the analysis of EH-TBB, FM550 and their potential metabolites are provided in Table SI-1.

Compound Discoverer 2.0 software (Thermo Fisher Scientific, Bremen, Germany) was used to detect potential metabolites and elucidate their chemical formulae, while quantification of target FRs was performed using Quan Browser 3.0 (Thermo Fisher Scientific, Bremen, Germany).

#### *QA/QC*

Metabolic activity of phases I enzymes including NADPH-cytochrome C reductase, carboxyl esterase and FMO3 were measured using guidelines and specific kits provided by Biopredic International and showed normal activities of all enzymes after HS-S9 thawing.

Quality assurance samples comprising William's E medium spiked with EH-TBB and FM550 mixture at all dosing levels were analyzed, with recoveries of dosing chemicals falling between 80 to 115% of the theoretical dosing concentrations. Internal standard recoveries in all HS-S9 incubation experiments ranged from 65-115%.

In all incubation experiments, a solvent blank comprising William's E medium was performed and analysed alongside the sample batch. No parent compounds or metabolites were found in solvent blanks with the exception of TPhP at negligible levels (< 1% of the lowest dosing level). Therefore, no blank correction was needed. Additionally, no metabolites were found in the non-enzymatic (all experimental components except HS-S9) and heat-inactivated (HS-S9 inactivated by heating at 70 °C for 30 min) controls run in parallel to each sample batch.

## Biotransformation kinetic modelling

The metabolite formation rate and substrate concentration of the studied chemicals were fitted to different biotransformation kinetic models (Northrop, 1983; Lipscomb and Poet, 2008) by nonlinear regression analysis using the SigmaPlot Enzyme Kinetics Module v.1.1 (Systat Software Inc., Richmond, CA) to determine the enzyme kinetic model that best describe the formation rates of the metabolites. The models used were the Michaelis-Menten equation (Equation 1), the Hill equation (Equation 2), and the substrate-inhibition kinetic equation (Equation 3) :

$$v = \frac{V_{\max} \times [S]}{K_m + [S]} \quad (\text{Equation 1})$$

$$v = \frac{V_{\max} \times [S]^n}{K' + [S]^n} \quad (\text{Equation 2})$$

$$v = \frac{V_{\max}}{1 + \frac{K_m}{[S]} + \frac{[S]}{K_i}} \quad (\text{Equation 3})$$

where  $v$  is initial velocity of the reaction,  $V_{\max}$  is the maximum metabolic rate,  $[S]$  is the substrate concentration,  $K_m$  is the Michaelis-Menten constant,  $K'$  is the Hill dissociation constant,  $n$  is the Hill coefficient and  $K_i$  is the inhibitory dissociation constant. Selection of the best fitted model was determined by statistical criteria to evaluate the goodness of the fit. The two statistical criteria used were Akaike Information Criterion corrected for small sample size (AICc) and the standard deviation of the residuals ( $Sy.x$ ). The model with the lowest values for AICc and for the standard deviation of the residuals was considered to be the model that best fit the data. When the formation rate of a primary metabolite is best described by the Michaelis-Menten model (Equation 1), the part of the *in vitro* intrinsic clearance ( $CL_{int,M}$ ) due to the formation of that metabolite can be calculated as follows:

$$CL_{int,M} = \frac{v}{[S]} = \frac{V_{\max}}{K_m + [S]} \quad (\text{Equation 4})$$

If the levels of the substrate of interest in human blood are negligible compared to the apparent  $K_m$  value associated with the formation of the metabolite, then  $(K_m + [S]) \approx K_m$  therefore Equation 4 can be written as follows (Lipscomb and Poet, 2008):

$$CL_{int} = \frac{v}{[S]} = \frac{V_{max}}{K_m} \quad (\text{Equation 5})$$

The total  $CL_{int}$  value of the substrate of interest can then be calculated as the sum of the  $CL_{int}$  of each of its primary metabolites.

The intrinsic *in vitro* clearance of a xenobiotic by an organ on kilogram human body weight ( $CL_{int-organ}$ ) basis can be scale up by the following equation:

$$CL_{int-organ} = CL_{int} \times p \times w \quad (\text{Equation 6})$$

Where  $p$  is the amount of protein per gram of an organ and  $w$  is the average weight of that organ per kilogram body weight.

The blood flow of an organ per kilogram body weight (kg b.w)  $Q_h$  was taken into account for extrapolation of *in vitro* clearance to *in vivo* clearance ( $CL_h$ ) as follows (Lipscomb and Poet, 2008):

$$CL_{organ} = \frac{Q_h \times CL_{int-organ}}{CL_{int-organ} + Q_h} \quad (\text{Equation 7})$$

## Results and Discussion

### *Dermal metabolic profiles of EH-TBB and FM550*

Due to the chemical structure of EH-TBB, BEH-TEBP and TPhP (Figure SI-1), we hypothesized that their metabolism by HS-S9 would be catalysed by carboxyesterases and/or cytochrome P450 enzymes. Full scan mode with either APCI or alternate switching positive/negative ESI ionization were used to screen for EH-TBB and FM550 dermal

metabolites. No potential metabolites were found in (+)ESI or (-)APCI mode. For EH-TBB samples, in (-)ESI mode there was one potential metabolite with the ion mass of 436.66814 and the proposed ion formula  $[C_7HBr_4O_2]^-$ . By comparing with the authentic standard, this was confirmed as the  $[M-H]^-$  molecular ion for TBBA (Figure 1). This is in agreement with the results of Roberts et al., who reported TBBA as the only *in vitro* metabolite of EH-TBB by human and rat liver microsomes (Roberts et al., 2012).

Following exposure of HS-S9 to FM550 mixture components, TBBA was also identified as the sole metabolite of EH-TBB. In addition, another potential metabolite with the ion mass of 249.03204 was detected in (-)ESI mode. The proposed chemical structure for this ion was  $[C_{12}H_{10}O_4P]^-$ . In order to elucidate the chemical structure of this compound, a MS/MS experiment was carried out in (-)ESI-SIM-MS<sup>2</sup> mode. A combination of low, medium and high collision energies were applied stepwise to achieve a diverse range of fragmentation ions. Specific Orbitrap-MS parameters for this experiment are provided in Table SI-2. The ion  $m/z = 249.03204$  was fragmented mainly into three ions: 154.98895, 93.03284 and 78.95728. The proposed chemical formula for these fragments were:  $[C_6H_4O_4P]^-$ ,  $[C_6H_5O]^-$  and  $[PO_3]^-$ , respectively (Figure 2). Based on the proposed parent ion formula and the MS<sup>2</sup> fragmentation data, this metabolite was identified as diphenyl phosphate (DPhP), assigned as a primary metabolite of TPhP. Metabolite identity was further confirmed via comparison and augmentation with an authentic chemical standard of DPhP. Previous studies have reported that *in vitro* metabolism of TPhP by human liver microsomes or chicken embryo hepatocytes formed DPhP, hydroxylated TPhP (OH-TPhP) and dihydroxylated TPhP ((OH)<sub>2</sub>-TPhP) (Van den Eede et al., 2013; Su et al., 2014). *In vivo* metabolism of TPhP in fish produced DPhP, OH-TPhP, (OH)<sub>2</sub>-TPhP and monophenyl phosphate among which DPhP

was the major metabolite (Wang et al., 2016). However, DPhP was detected as the sole metabolite of TPhP by HS-S9 in the present study.

By comparison of the *in vitro* human dermal (this study) and hepatic metabolic profiles of EH-TBB and TPhP,(Roberts et al., 2012; Van den Eede et al., 2013) it was obvious that the oxidative metabolites could not be identified in the HS-S9 experiments under the current experimental conditions. Proteomic profiling of the metabolic activity of dermal HS-S9 fractions show that both CYP450 and carboxylesterases are active, albeit at much lower levels than in the liver cells (Oesch et al., 2018). Moreover, the reported levels of CYP450 enzymes in human skin were at least 300 fold lower than that in human liver. In contrast, the relative level of carboxylesterase 1 (CES1) in human skin and liver was 0.62 with no significant level difference ( $P = 0.21$ ) (van Eijl et al., 2012). Such low level of CYP450 enzymes and similar level of CES1 in the skin in comparison with liver might explain why no oxidative metabolites were observed in the present study. To test this hypothesis, we performed NADPH-independent (i.e. without NADPH cofactor) *in vitro* incubation of EH-TBB and FM550 with HS-S9 under the same conditions. The absence of NADPH did not result in significant changes in the formation rates of TBBA, DPhP or depletion rates of the parent compounds ( $P>0.05$ ). These results reveal differences from hepatic metabolism as dermal carboxylesterases seem to be the major metabolizing enzymes of the target FRs in human skin. This does not eliminate the possibility of oxidative metabolite formation upon dermal contact under real-life situations (i.e. upon exposure to larger doses) but if formed, they are likely to be at lower rates and concentrations than de-esterified metabolites.

Finally, no stable metabolites of BEH-TEBP were identified in HS-S9 exposed to FM550 mixture at any of the studied concentrations (0.3 – 4.5  $\mu$ M – Table SI-2), despite the high

sensitivity and selectivity of the Orbitrap-MS platform applied in this study. This is in agreement with the results of Roberts et al. who did not detect any metabolites for BEH-TEBP in human and rat hepatic subcellular fractions. Interestingly, mono(2-ethylhexyl) tetrabromophthalate, was only detected in purified hepatic porcine carboxylesterase, although at a very slow formation rate of  $1.08 \text{ pmol min}^{-1} \text{ mg protein}^{-1}$  (Roberts et al., 2012). This may reflect inter-species variation in the biotransformation of this flame retardant and warrants further studies to elucidate the hepatic and extrahepatic metabolic profiles of BEH-TEBP in human.

#### *Biotransformation kinetics of EH-TBB and FM 550 by HS-S9*

In a previous communication, our research group reported the hepatic metabolic rates of the brominated FR, 1,2-dibromo-4-(1,2 dibromoethyl) cyclohexane (TBECH), were largely dependent on whether the metabolizing enzymes were challenged with a single compound or a mixture of components (Nguyen et al., 2017). Therefore, a series of incubation experiments of HS-S9 with different concentrations of EH-TBB and FM550 components (Table SI-3) were performed. With these experiments, we aimed to investigate whether the metabolic rate will be different upon challenging the HS-S9 with a multi-component mixture representing FM550 (i.e. mimicking real-life situation) compared to exposure to a single flame retardant (EH-TBB). The concentrations of TBBA and DPhP were quantified using isotope dilution series method with  $^{13}\text{C}$ -TBBA and  $\text{d}_{15}$ -TPhP as internal (surrogate) standards. The results from kinetic modelling in SigmaPlot® software revealed the formation of TBBA in both pure EH-TBB and FM550 mixture experiments was best fitted by the Michaelis-Menten model (Figure 3). The model-derived kinetic parameters for the formation of TBBA are presented in Table 1. Estimated maximum metabolic rate ( $V_{\text{max}}$ ) for

the formation of TBBA upon exposure to FM550 mixture was significantly lower ( $p < 0.05$ ) than  $V_{\max}$  upon exposure to individual EH-TBB (1.80 and 15.2  $\mu\text{mol min}^{-1} \text{mg protein}^{-1}$ , respectively). However, in both cases,  $V_{\max}$  was substantially less than that reported previously for EH-TBB metabolism by human liver microsomes (644  $\mu\text{mol min}^{-1} \text{mg protein}^{-1}$ ) (Roberts et al., 2012). The estimated Michaelis constant ( $K_m$ ) for FM550 is lower than  $K_m$  for EH-TBB metabolism by HS-S9 (Table 1). Such significant decreases in both  $K_m$  and  $V_{\max}$  suggest that the rate of metabolite formation (TBBA) from FM550 by HS-S9 has potentially been influenced by competitive substrate inhibition. The competitive inhibitors could be BEH-TEBP and/or TPhP in the FM550 dosing solutions.

The formation rate of DPhP (primary metabolite of TPhP) did not fit any of the assessed enzyme kinetic models (Michaelis-Menten, Hill or substrate-inhibition). Indeed, it did not show any signs of reaching a plateau to indicate a steady state was reached. Another series of incubation experiments with higher doses of FM550 were carried out at equivalent TPhP concentrations of 16.8, 25 and 33.6  $\mu\text{M}$ . Close to linearity increment of DPhP formation rate was still observed and steady state conditions could not be achieved. This observation is in agreement with a previous study on TPhP biotransformation in human serum, where the formation rate of DPhP did not reach a plateau even at concentrations up to 100  $\mu\text{M}$  of TPhP (Van den Eede et al., 2016). The lack of fit to the investigated kinetic models precluded the estimation of metabolic kinetic parameters for TPhP under the applied experimental conditions.

#### *In vitro – in vivo extrapolation for dermal clearance of EH-TBB*

As the formation rates of TBBA were best described by the Michaelis-Menten model, the model was applied to estimate *in vivo* dermal clearance of EH-TBB assuming average adult



bodyweight of 70 kg. We then compared our results for dermal clearance to those reported previously by Roberts et al. for human hepatic clearance of EH-TBB (Roberts et al., 2012). The following parameters were applied: 24.84 mg protein/g skin for HS-S9 (calculated as total of microsomes and cytosol),(Jewell et al., 2007) 37 g skin/kg bodyweight, 52.5 mg protein/g liver for HLM, 25.7 g liver/kg bodyweight,  $Q_h = 20.7$  mL/min/kg bodyweight and  $Q_{skin} = 4.37$  mL/min/kg bodyweight (Manevski et al., 2015). Our model calculations estimated *in vivo* dermal clearance of individual EH-TBB and EH-TBB in FM-550 to be 0.48 and 0.92 mL/min/kg bodyweight, respectively (Table 2). These rates were much smaller than the skin blood flow (4.37 mL/min/kg bodyweight), suggesting EH-TBB is not readily cleared by dermal metabolism and is likely to accumulate in the skin tissue. Indeed, the extraction ratios (defined as the ratio between the *in vivo* clearance of a xenobiotic to the blood flow for a specific organ)(Manevski et al., 2015) of EH-TBB by human skin were only 11% and 21% for individual and mixture exposures, respectively. This is also in agreement with the results of Frederiksen et al. (2016) who reported the accumulation of EH-TBB in the skin using a human *ex vivo* dermal model. In contrast, human liver showed higher EH-TBB extraction ratio up to 80% with *in vivo* hepatic clearance of 16.4 mL/min/kg bodyweight (Table 2). These results suggested that dermal metabolism contributed marginally to the clearance of internal EH-TBB body burden in comparison with liver metabolism.

### *Study limitations*

It is important to note that due to limited availability, the skin HS-S9 applied in this study was pooled from the abdominal skin of 3 white female donors (age range 33-46 years). The dermal metabolic activity may vary widely depending on age, race, gender and skin

location (Oesch et al., 2018). Additionally, our *in vitro* – *in vivo* metabolic clearance calculations were based on the assumption that the unbound fraction of chemical pollutant to blood proteins equals 1, meaning all EH-TBB in the blood was free and available for metabolism. This can cause overestimation of the estimated xenobiotic clearance. Furthermore, TBBA was treated as the only primary metabolite of EH-TBB. While our experimental measurements support this assumption, it is possible that other metabolites (e.g. oxidative or debrominated metabolites) may be formed under real conditions of prolonged skin contact with high concentration of EH-TBB (e.g. sleeping on a flame retarded mattress). The potential formation of other primary metabolites under different conditions may also influence the estimated metabolic rates for EH-TBB in the current study.

#### *Implications for human exposure*

Even though the outer most layer of skin (*stratum corneum*) serves as a barrier to prevent unwanted chemicals from entering the human body, recent studies have confirmed the dermal uptake of several lipophilic pollutants such as hexabromocyclododecanes (HBCDDs), tetrabromobisphenol-A (TBBPA), organophosphate flame retardants or novel brominated flame retardants via contact with skin (Abdallah et al., 2015; Abdallah et al., 2016; Frederiksen et al., 2016; Knudsen et al., 2017). Frederiksen et al. reported roughly 10% dermal absorption and 0.1 - 0.2% penetration of several FRs including EH-TBB following a single dose (of several hundred nanograms) application to *ex vivo* human skin for 72 h (Frederiksen et al., 2016). Higher dermal uptake at 20% with 0.2% penetration of administered <sup>14</sup>C-labelled EH-TBB to *in vitro* human skin after 24 h exposure was also reported (Knudsen et al., 2016). Nevertheless, it is proven that EH-TBB as well as other

organic FRs can penetrate the skin barrier and be “trapped” within the skin tissue until reaching the blood circulation (i.e. become bioavailable). In such an event, skin metabolism may play an important role in the clearance of the trapped dose within the skin tissue, yet it may also help create a concentration gradient through the different layers of the skin tissue to facilitate further uptake of the parent FR. Moreover, the slow *in vitro* clearance rates in the skin could translate into slow EH-TBB *in vivo* percutaneous metabolism and subsequently result in inefficient removal of EH-TBB from the skin. This partially explains the reported accumulation of EH-TBB in the skin tissue prior to reaching the systemic circulation (Knudsen et al., 2016). In addition, very little is known about the toxicokinetics and toxicodynamics of the dermal biotransformation products (i.e. TBBA and DPhP). This is of concern as these metabolites may lead to potential adverse health effects similar to that reported previously for PBDE metabolites (Saqib et al., 2018). Therefore, further studies on dermal uptake and metabolism of emerging flame retardants are required to fully understand both the toxicological and exposure implications of dermal biotransformation of these hazardous chemicals.

## Acknowledgement

The authors acknowledge gratefully the assistance of Mrs Adriana Carolina Torres Moreno of the University of Cartagena, Colombia. This research received funding from the European Union's Horizon 2020 research and innovation programme under the Marie Skłodowska-Curie grant agreement No 734522 (INTERWASTE project). It also received funding from the European Union Seventh Framework Programme FP7/ 2007-2013 under grant agreement No. 606857 (ELUTE project).

409

## 410 **Supporting information**

411 Details of analytical method parameters and metabolite identification workflow are  
412 provided as supporting information.

413

## 414 **References**

415 Abdallah, M.A., Pawar, G., Harrad, S., 2016. Human dermal absorption of chlorinated  
416 organophosphate flame retardants; implications for human exposure. *Toxicology and*  
417 *Applied Pharmacology* 291, 28-37.

418 Abdallah, M.A.E., Harrad, S., 2018. Dermal contact with furniture fabrics is a significant  
419 pathway of human exposure to brominated flame retardants. *Environ Int* 118, 26-33.

420 Al-Omran, L.S., Harrad, S., 2016. Distribution pattern of legacy and "novel" brominated  
421 flame retardants in different particle size fractions of indoor dust in Birmingham, United  
422 Kingdom. *Chemosphere* 157, 124-131.

423 Belcher, S.M., Cookman, C.J., Patisaul, H.B., Stapleton, H.M., 2014. In vitro assessment of  
424 human nuclear hormone receptor activity and cytotoxicity of the flame retardant mixture  
425 FM 550 and its triarylphosphate and brominated components. *Toxicology Letters* 228, 93-  
426 102.

427 Basis, A., Christia, C., Poma, G., Covaci, A., Samara, C., 2017. Legacy and novel brominated  
428 flame retardants in interior car dust - Implications for human exposure. *Environmental*  
429 *Pollution* 230, 871-881.

430 Carignan, C.C., Heiger-Bernays, W., McClean, M.D., Roberts, S.C., Stapleton, H.M., Sjodin, A.,  
431 Webster, T.F., 2013. Flame Retardant Exposure among Collegiate United States Gymnasts.  
432 *Environmental Science & Technology* 47, 13848-13856.

433 Cequier, E., Ionas, A.C., Covaci, A., Marce, R.M., Becher, G., Thomsen, C., 2014. Occurrence of  
434 a Broad Range of Legacy and Emerging Flame Retardants in Indoor Environments in  
435 Norway. *Environmental Science & Technology* 48, 6827-6835.

436 Dodson, R.E., Perovich, L.J., Covaci, A., Van den Eede, N., Ionas, A.C., Dirtu, A.C., Brody, J.G.,  
 437 Rudel, R.A., 2012. After the PBDE Phase-Out: A Broad Suite of Flame Retardants in Repeat  
 438 House Dust Samples from California. *Environmental Science & Technology* 46, 13056-  
 439 13066.

440 Frederiksen, M., Stapleton, H.M., Vorkamp, K., Webster, T.F., Jensen, N.M., Sorensen, J.A.,  
 441 Nielsen, F., Knudsen, L.E., Sorensen, L.S., Clausen, P.A., Nielsen, J.B., 2018. Dermal uptake  
 442 and percutaneous penetration of organophosphate esters in a human skin ex vivo model.  
 443 *Chemosphere* 197, 185-192.

444 Frederiksen, M., Vorkamp, K., Jensen, N.M., Sorensen, J.A., Knudsen, L.E., Sorensen, L.S.,  
 445 Webster, T.F., Nielsen, J.B., 2016. Dermal uptake and percutaneous penetration of ten flame  
 446 retardants in a human skin ex vivo model. *Chemosphere* 162, 308-314.

447 Hammel, S.C., Hoffman, K., Lorenzo, A.M., Chen, A., Phillips, A.L., Butt, C.M., Sosa, J.A.,  
 448 Webster, T.F., Stapleton, H.M., 2017. Associations between flame retardant applications in  
 449 furniture foam, house dust levels, and residents' serum levels. *Environment International*  
 450 107, 181-189.

451 Hopf, N.B., Berthet, A., Vernez, D., Langard, E., Spring, P., Gaudin, R., 2014. Skin permeation  
 452 and metabolism of di(2-ethylhexyl) phthalate (DEHP). *Toxicology Letters* 224, 47-53.

453 Jewell, C., Ackermann, C., Payne, N.A., Fate, G., Voorman, R., Williams, F.M., 2007. Specificity  
 454 of procaine and ester hydrolysis by human, minipig, and rat skin and liver. *Drug*  
 455 *Metabolism and Disposition* 35, 2015-2022.

456 Knudsen, G.A., Hughes, M.F., Sanders, J.M., Hall, S.M., Birnbaum, L.S., 2016. Estimation of  
 457 human percutaneous bioavailability for two novel brominated flame retardants, 2-  
 458 ethylhexyl 2,3,4,5-tetrabromobenzoate (EH-TBB) and bis(2-ethylhexyl)  
 459 tetrabromophthalate (BEH-TEBP). *Toxicology and Applied Pharmacology* 311, 117-127.

460 Lipscomb, J.C., Poet, T.S., 2008. In vitro measurements of metabolism for application in  
 461 pharmacokinetic modeling. *Pharmacology & Therapeutics* 118, 82-103.

462 Ma, Y.N., Venier, M., Hites, R.A., 2012. 2-Ethylhexyl Tetrabromobenzoate and Bis(2-  
 463 ethylhexyl) Tetrabromophthalate Flame Retardants in the Great Lakes Atmosphere.  
 464 *Environmental Science & Technology* 46, 204-208.

465 Manevski, N., Swart, P., Balavenkatraman, K.K., Bertschi, B., Camenisch, G., Kretz, O., Schiller,  
 466 H., Walles, M., Ling, B., Wettstein, R., Schaefer, D.J., Itin, P., Ashton-Chess, J., Pognan, F., Wolf,

467 A., Litherland, K., 2015. Phase II Metabolism in Human Skin: Skin Explants Show Full  
 468 Coverage for Glucuronidation, Sulfation, N-Acetylation, Catechol Methylation, and  
 469 Glutathione Conjugation. *Drug Metabolism and Disposition* 43, 126-139.

470 Mankidy, R., Ranjan, B., Honaramooz, A., Giesy, J.P., 2014. Effects of novel brominated flame  
 471 retardants on steroidogenesis in primary porcine testicular cells. *Toxicology Letters* 224,  
 472 141-146.

473 Nguyen, K.H., Abdallah, M.A.E., Moehring, T., Harrad, S., 2017. Biotransformation of the  
 474 Flame Retardant 1,2-Dibromo-4-(1,2-dibromoethyl)cyclohexane (TBECH) in Vitro by  
 475 Human Liver Microsomes. *Environmental Science & Technology* 51, 10511-10518.

476 Northrop, D.B., 1983. FITTING ENZYME-KINETIC DATA TO V/K. *Anal. Biochem.* 132, 457-  
 477 461.

478 Oesch, F., Fabian, E., Landsiedel, R., 2018. Xenobiotica-metabolizing enzymes in the skin of  
 479 rat, mouse, pig, guinea pig, man, and in human skin models. *Archives of Toxicology* 92,  
 480 2411-2456.

481 Patisaul, H.B., Roberts, S.C., Mabrey, N., McCaffrey, K.A., Gear, R.B., Braun, J., Belcher, S.M.,  
 482 Stapleton, H.M., 2013. Accumulation and Endocrine Disrupting Effects of the Flame  
 483 Retardant Mixture Firemaster (R) 550 in Rats: An Exploratory Assessment. *Journal of*  
 484 *Biochemical and Molecular Toxicology* 27, 124-136.

485 Pillai, H.K., Fang, M.L., Beglov, D., Kozakov, D., Vajda, S., Stapleton, H.M., Webster, T.F.,  
 486 Schlezinger, J.J., 2014. Ligand Binding and Activation of PPAR gamma by Firemaster (R)  
 487 550: Effects on Adipogenesis and Osteogenesis in Vitro. *Environmental Health Perspectives*  
 488 122, 1225-1232.

489 Roberts, S.C., Macaulay, L.J., Stapleton, H.M., 2012. In Vitro Metabolism of the Brominated  
 490 Flame Retardants 2-Ethylhexyl-2,3,4,5-Tetrabromobenzoate (TBB) and Bis(2-ethylhexyl)  
 491 2,3,4,5-Tetrabromophthalate (TBPH) in Human and Rat Tissues. *Chemical Research in*  
 492 *Toxicology* 25, 1435-1441.

493 Saquib, Q., Siddiqui, M.A., Ahmad, J., Ansari, S.M., Al-Wathnani, H.A., Rensing, C., 2018. 6-  
 494 OHBDE-47 induces transcriptomic alterations of CYP1A1, XRCC2, HSPA1A, EGR1 genes and  
 495 trigger apoptosis in HepG2 cells. *Toxicology* 400, 40-47.

496 Saunders, D.M.V., Higley, E.B., Hecker, M., Mankidy, R., Giesy, J.P., 2013. In vitro endocrine  
 497 disruption and TCDD-like effects of three novel brominated flame retardants: TBPH, TBB, &  
 498 TBCO. *Toxicology Letters* 223, 252-259.

499 Strid, A., Bruhn, C., Sverko, E., Svavarsson, J., Tomy, G., Bergman, A., 2013. Brominated and  
 500 chlorinated flame retardants in liver of Greenland shark (*Somniosus microcephalus*).  
 501 *Chemosphere* 91, 222-228.

502 Stubbings, W.A., Schreder, E.D., Thomas, M.B., Romanak, K., Venier, M., Salamova, A., 2018.  
 503 Exposure to brominated and organophosphate ester flame retardants in US childcare  
 504 environments: Effect of removal of flame-retarded nap mats on indoor levels.  
 505 *Environmental Pollution* 238, 1056-1068.

506 Su, G.Y., Crump, D., Letcher, R.J., Kennedy, S.W., 2014. Rapid in Vitro Metabolism of the  
 507 Flame Retardant Triphenyl Phosphate and Effects on Cytotoxicity and mRNA Expression in  
 508 Chicken Embryonic Hepatocytes. *Environmental Science & Technology* 48, 13511-13519.

509 Tao, F., Abdallah, M.A., Ashworth, D.C., Douglas, P., Toledano, M.B., Harrad, S., 2017.  
 510 Emerging and legacy flame retardants in UK human milk and food suggest slow response to  
 511 restrictions on use of PBDEs and HBCDD. *Environment International* 105, 95-104.

512 Tao, F., Abdallah, M.A.E., Harrad, S., 2016. Emerging and Legacy Flame Retardants in UK  
 513 Indoor Air and Dust: Evidence for Replacement of PBDEs by Emerging Flame Retardants?  
 514 *Environmental Science & Technology* 50, 13052-13061.

515 Van den Eede, N., Ballesteros-Gomez, A., Neels, H., Covaci, A., 2016. Does Biotransformation  
 516 of Aryl Phosphate Flame Retardants in Blood Cast a New Perspective on Their Debated  
 517 Biomarkers? *Environmental Science & Technology* 50, 12439-12445.

518 Van den Eede, N., Maho, W., Erratico, C., Neels, H., Covaci, A., 2013. First insights in the  
 519 metabolism of phosphate flame retardants and plasticizers using human liver fractions.  
 520 *Toxicology Letters* 223, 9-15.

521 van Eijl, S., Zhu, Z.Y., Cupitt, J., Gierula, M., Gotz, C., Fritsche, E., Edwards, R.J., 2012.  
 522 Elucidation of Xenobiotic Metabolism Pathways in Human Skin and Human Skin Models by  
 523 Proteomic Profiling. *Plos One* 7.

524 Wang, G.W., Du, Z.K., Chen, H.Y., Su, Y., Gao, S.X., Mao, L., 2016. Tissue-Specific Accumulation,  
 525 Depuration, and Transformation of Triphenyl Phosphate (TPHP) in Adult Zebrafish (*Danio*  
 526 *rerio*). *Environmental Science & Technology* 50, 13555-13564.

Xu, F.C., Garcia-Bermejo, A., Malarvannan, G., Gomara, B., Neels, H., Covaci, A., 2015. Multi-contaminant analysis of organophosphate and halogenated flame retardants in food matrices using ultrasonication and vacuum assisted extraction, multi-stage cleanup and gas chromatography-mass spectrometry. *Journal of Chromatography A* 1401, 33-41.

Zheng, X.B., Xu, F.C., Luo, X.J., Mai, B.X., Covaci, A., 2016. Phosphate flame retardants and novel brominated flame retardants in home-produced eggs from an e-waste recycling region in China. *Chemosphere* 150, 545-550.



## Tables

Table 1: Kinetic parameters derived from Michaelis-Menten model for the formation of TBBA following incubation of HS-S9 with pure EH-TBB and FM550 mixture in the present study compared to the reported parameters for EH-TBB incubation with human liver microsomes (HLM).(Roberts et al., 2012)

Substrate	Model	$K_m$ ( $\mu$ M) $\pm$ standard deviation	$V_{max}$ (pmol/min/mg protein) $\pm$ standard deviation
<b>EH-TBB</b>	HS-S9	$4.57 \pm 1.2$	$15.2 \pm 5$
<b>FM550</b>	HS-S9	$0.84 \pm 0.19$	$1.80 \pm 0.05$
<b>EH-TBB</b>	HLM	$11.1 \pm 3.9$	$644 \pm 144$

Table 2: Estimated *in vitro* and *in vivo* clearance of EH-TBB by human skin (the current study) compared to those reported in human liver (Roberts et al., 2012).

Chemical	Organ	$CL_{int-organ}$ ( <i>in vitro</i> , mL/min/kg b.w)	$CL_{organ}$ ( <i>in vivo</i> , mL/min/kg b.w)
<b>EH-TBB</b>	Skin	0.54	0.48
<b>EH-TBB in FM550</b>	Skin	1.18	0.92
<b>EH-TBB</b>	Liver	78.3	16.4

## Figures

Figure 1: TBBA detected as the sole metabolite of EH-TBB in Human Skin S9 fraction (HS-S9) exposed to 10  $\mu$ M of EH-TBB.  $^{13}\text{C}$ -TBBA is the isotope-labelled form used for identity confirmation and quantification of TBBA.

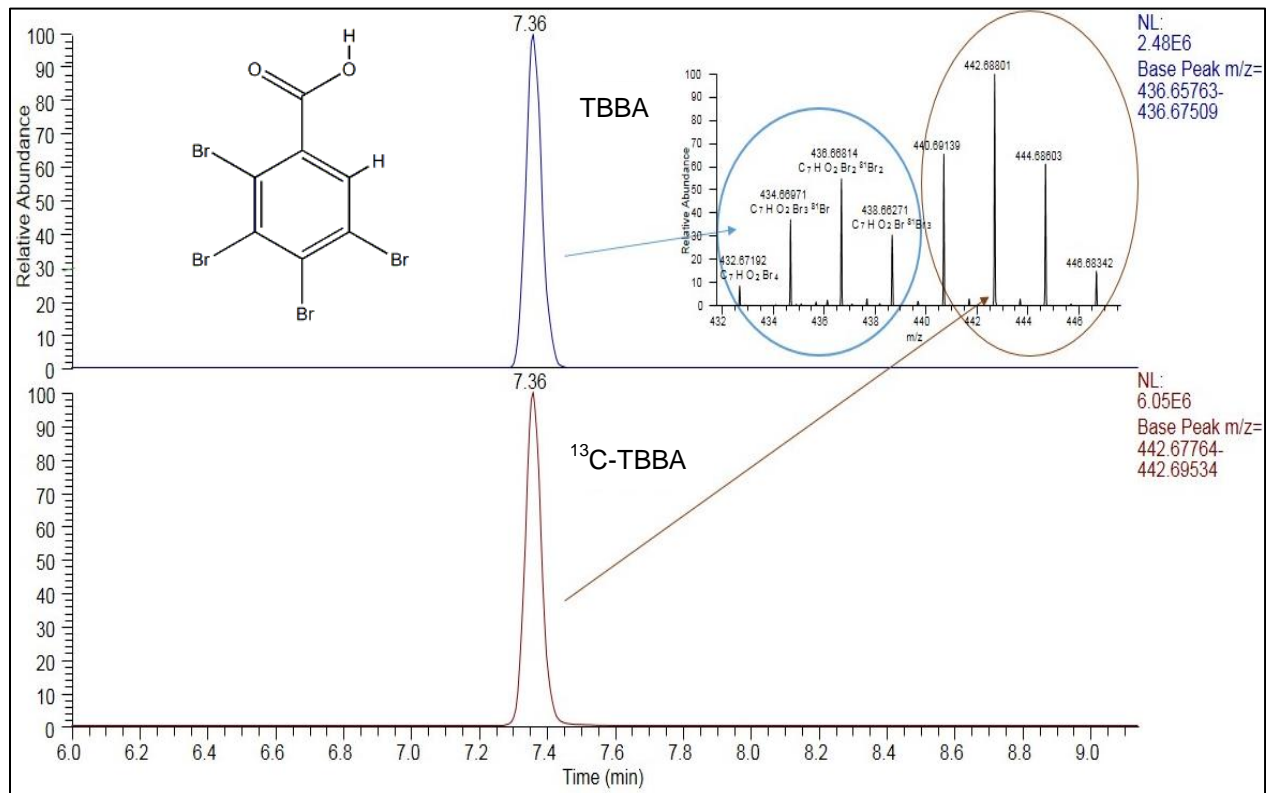


Figure 2: (-)ESI-MS/MS<sup>2</sup> spectrum of the ion 249.03204 by UPLC-Orbitrap HRMS

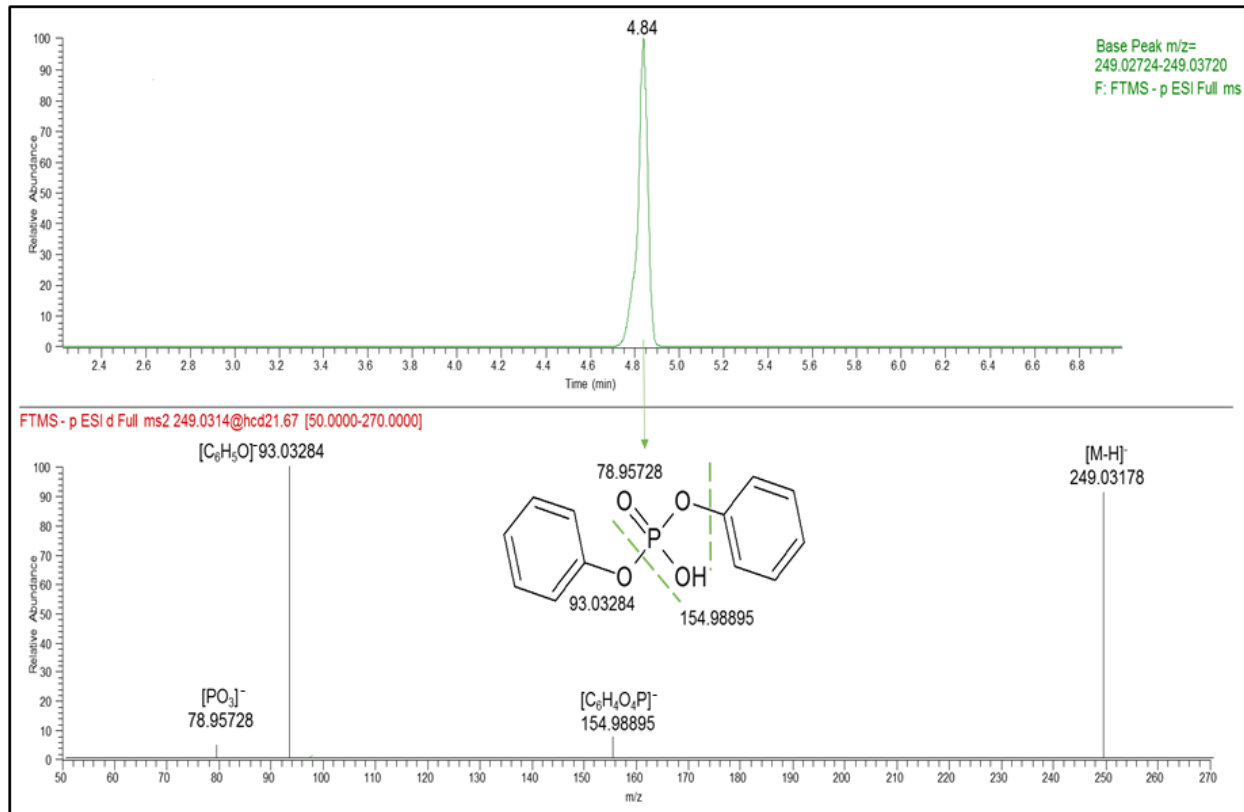


Figure 3: Kinetics of TBBA formation in EH-TBB (A) and FM550 mixture (B) incubation experiments with HS-S9 using the Michaelis-Menten model. Error bars represent 1 standard deviation (n=3).

